General and Comparative Endocrinology 277 (2019) 122–129

Contents lists available at ScienceDirect

General and Comparative Endocrinology

journal homepage: www.elsevier.com/locate/ygcen

Loss of Gsdf leads to a dysregulation of Igf2bp3-mediated oocyte development in medaka

Xiaowen Wu[a,b,1], Yingqing Zhang[a,b,1], Shumei Xu[a,b,1], Yuyang Chang[a,b], Yang Ye[c], Anning Guo[a,b], Yi Kang[a,b], Haiyan Guo[a,b], Hongyan Xu[d], Liangbiao Chen[a,b], Xiaomiao Zhao[c,*], Guijun Guan[a,b,*]

[a] Key Laboratory of Exploration and Utilization of Aquatic Genetic Resources, Ministry of Education, Shanghai 201306, China
[b] Shanghai Collaborative Innovation for Aquatic Animal Genetics and Breeding, College of Fisheries and Life Sciences, Shanghai Ocean University, Shanghai 201306, China
[c] Department of Obstetrics and Gynecology, Sun Yat-sen Memorial Hospital, Sun Yat-sen University Yanjiang Road 107, Guangdong 510120, China
[d] Key Laboratory of Tropical and Subtropical Fishery Resource Application and Cultivation of Ministry of Agriculture, Pearl River Fisheries Research Institute, Chinese Academy of Fishery Sciences, Guangzhou 51-380, China

ARTICLE INFO

Keywords:
Gonadal soma-derived factor (Gsdf)
Insulin-like growth factor 2 mRNA binding protein 3 (Igf2bp3)
Trimethylated histone H3 lysine 27 (H3K27me3)

ABSTRACT

Gonadal soma-derived factor (Gsdf) is a unique TGF-β factor essential for both ovarian and testicular development in Hd-rR medaka (*Oryzias latipes*). However, the downstream genes regulated by Gsdf signaling remain unknown. Using a high-throughput proteomic approach, we identified a significant increase in the expression of the RNA-binding protein Igf2bp3 in *gsdf*-deficient ovaries. We verified this difference in transcription and protein expression against normal gonads using real-time PCR quantification and Western blotting. The genomic structure of *igf2bp3* and the syntenic flanking segments are highly conserved across fish and mammals. *igf2bp3* expression was correlated with oocyte development, which is consistent with the expression of the *igf2bp3* ortholog Vg1-RBP/Vera in *Xenopus*. In contrast to the normal ovary, cysts of H3K27me3- and Igf2bp3-positive germ cells were dramatically increased in the one-month-old *gsdf*-deficient ovary, indicating that the *gsdf* depletion led to a dysregulation of Igf2bp3-mediated oocyte development. Our results provide novel insights into the Gsdf-Igf2bp3 signaling mechanisms that underlie the fundamental process of gametogenesis; these mechanisms may be well conserved across phyla.

1. Introduction

Gonadal soma-derived factor (*gsdf*) plays an essential role in the development of both the testis and the ovary, as demonstrated by the gain- and loss-of-function in the medaka (Jananese rice fish; *Oryzias latipes*) (Zhang et al., 2016). The expression of *gsdf* was co-localized and regulated by the master sex-determining gene *dmy* (also known as *dmrt1bY*) during the initiation of morphological testicular differentiation (Matsuda et al., 2002; Nanda et al., 2002; Shibata et al., 2010). Importantly, *gsdf* depletion leads to an excessive proliferation of germ cells during sexual differentiation, regardless of sex (XX or XY) (Imai et al., 2015; Zhang et al., 2016). Thus, *gsdf* knockout (*gsdf* KO) ovaries are hypertrophic, with numerous primary oocytes (Guan et al., 2017). This ovarian phenotype resembles those of anti-Müllerian hormone receptor II knockout (*amhr2* KO, *hotei* mutant) (Morinaga et al., 2007), follicular stimulating hormone knockouts (*fsh* KO) (Takahashi et al., 2016), and follicular stimulating hormone receptor knockouts (*fshr* KO) (Murozumi et al., 2014). The C-terminal TGF-β domains of the Gsdf and Amh proteins are highly homologous and have similar expression patterns during sexual differentiation (Shibata et al., 2010; Zhu et al., 2016). Moreover, *gsdf* deletion leads to a downregulation of *fshr* in medaka gonads (Sun et al., 2017), suggesting that Gsdf, Amh and Fshr are involved in the principal pathway of germ cell development. However, the molecular mechanisms underlying the roles of these proteins in gametogenesis remain elusive.

In medaka, germ cells have an inherent feminizing effect (Nishimura et al., 2018). Thus, germ cells drive their own sexual differentiation (Nishimura et al., 2015, 2018), independent of the somatic *dmy* master sex-determining gene (Matsuda et al., 2002; Nanda et al., 2002). Disruption of the germ cell-intrinsic sex-determining factor

* Corresponding authors at: College of Fisheries and Life Sciences, Shanghai Ocean University, HuchengHuan Road 999, Shanghai 201306, China (G. Guan). Reproductive Endocrinology & Infertility, Sun Yat-sen Memorial Hospital, Sun Yat-sen University, Yanjiang Road 107, Guangzhou, Guangdong 510120, China (X. Zhao).
E-mail addresses: zhxmiao@mail.sysu.edu.cn (X. Zhao), gjguan@shou.edu.cn (G. Guan).
[1] These authors contributed equally.

https://doi.org/10.1016/j.ygcen.2019.04.001
Received 24 January 2019; Received in revised form 20 March 2019; Accepted 1 April 2019
Available online 02 April 2019

Forkhead box L3 (*foxl3*) induces the development of functional sperm in the female gonadal environment (Nishimura et al., 2015). Depletion of *gsdf* increases the number of germ cells sufficient for male-to-female sex reversal in XY medaka (Imai et al., 2015; Nishimura et al., 2018; Zhang et al., 2016). Thus, in medaka, the feminizing effects of the germ cells (derived from primordial germ cells, PGCs) may be activated during gonocyte formation when *gsdf* is depleted (Nishimura et al., 2018). However, it remains unclear how somatic sex-determining signaling coordinates the germ cell-intrinsic cues that lead to germ cell differentiation.

The protein networks underlying the sex reversal of swamp eel can be systematically identified on a quantitative analysis of protein expression from high-resolution, comprehensive proteomic databases (Sheng et al., 2015). Proteomics supports the characterization of biological outcomes and allows alterations in key factors to be identified via the annotation of proteins significantly differentially in experimental groups as compared to control groups (Zhu et al., 2010). In this study, we used proteomics to isolate the RNA-binding protein Igf2bp3, which was highly expressed in *gsdf*-deficient XY ovaries, as compared to normal female and male gonads. We used reverse transcription-polymerase chain reactions (RT PCRs), real-time PCRs (qPCRs), and Western blots to show that *igf2bp3* gene transcription and translation were greater in *gsdf*-deficient ovaries than in normal ovaries. We found that *gsdf*-depletion led to an abnormal increase of cystic germ cells growing in one-month-old XY ovary, with high *igf2bp3* expression in some zygotene and pachytene oocytes, but *igf2bp3*-silencing in the gonocytes and other pachytene oocytes within the same cyst. Therefore at least two populations of oocytes were developed after the onset of meiosis in *gsdf* KO ovary. Our results suggested that *gsdf-igf2bp3* played an essential role in germ cell differentiation during mitosis-meiosis transition in medaka.

2. Materials and methods

2.1. Sample preparation, and protein digestion for label-free proteomic analysis

Hd-rR strain was used in this experiment and housed in re-circulating systems at 26–28 °C, with a 14-h light/10-h dark photoperiod. All of the fish were handled following the guidelines of the Committee for Laboratory Animal Research at Shanghai Ocean University (Shanghai, China). From each group (wild-type ovary, wild-type testis and *gsdf*-deficient ovary), we selected 7 ~ 10 fish to serve as a pooled sample, in order to minimize individual differences. Sex genotyping was performed with PCR to amplify a *dmy*-specific fragment and a *dmrt1* fragment (Matsuda et al., 2002), and *gsdf* alleles described previously (Zhang et al., 2016).

Pooled samples were homogenized in liquid nitrogen and extracted with lysis buffer [8 M urea, 100 mM Tris-HCl, and 1% (v/v) cOmplete™ Protease Inhibitor Cocktail (Roche Diagnostics, Basel, Switzerland)]. The supernatants were collected from lysates after being sonicated, centrifuged, and subcequently reduced using 5 mM dithiothreitol (DTT) at 37 °C for 45 min and alkylated using 20 mM iodoacetamide (IAA) at room temperature (RT) for 30 min in the dark. Protein concentrations were measured using Bradford protein assay kits (Biyuntian, Shanghai, China). All of the protein samples were digested on filters with trypsin (Sigma-Aldrich, St. Louis, MO), at a 1:50 trypsin to protein ratio, at 37 °C for 12 h. Digested fractions were collected and stored at −80 °C for proteomics analysis. Three sets of samples (representing three biological replicates) were analyzed independently for each group, yielding a total of nine biological samples.

2.2. Label-free mass spectrometry

Label-free proteomics was performed by the Beijing Bangfei Bioscience Co., Ltd. (Beijing, China). Enzyme specificity was set to trypsin, and a maximum of two missed cleavages were allowed. The mass tolerance for precursor ions was set to 20 parts per million (ppm) in the first search and 5 ppm in the main search; and the mass tolerance for fragment ions was set to 0.02 Da. A carbamidomethyl group on cysteine was specified as a fixed modification, while oxidation and N-terminal acetylation were specified as variable modifications. Protein abundance among the samples was determined using label-free quantification (LFQ), with the false discovery rate (FDR; calculated as N (decoy)*(N(decoy) + N(target)) threshold set to < 1%, and the expected ion score cut-off set to < 0.05 (95% confidence).

2.3. Bioinformatics data analysis and protein identification

Raw data were converted to Mascot generic peak lists using the Maxquant search engine (v.1.5.2.8). Tandem mass spectra were searched against *O. latipes* sequence database (UP000001038, 26,094 entries) using mascot 2.0 (Matrix Science, London, UK). Both peptide and protein identifications were filtered using a cutoff of 1% for the peptide false identification rate (FDR). The minimum and maximum peptide lengths were set to 6 and 144 amino acids, respectively. Proteins containing more than one unique peptide were considered unique.

2.4. qPCR amplification and Western blots

Total RNAs were extracted from multiple tissues and reverse-transcribed into first-strand cDNA using AMV reverse transcriptase (Takara, Dalian, China), and oligo-dT(18) primers (Shenggong Co. Ltd., Shanghai, China), following the manufacturer's instructions. qPCR was performed using cDNA as template, with SYBR Fast qPCR mix (Takara, Dailian, China) on a 7500 real-time PCR system (Applied Biosystems, Foster City, CA). The housekeeping gene β-actin was used to normalize expression values. Statistical significance was determined using pairwise Student's *t*-tests. We considered $p < 0.05$ to be statistically significant. Data are presented as mean values ± standard error of six individuals' adult gonads.

Gonadal proteins were separated on 10% dodecyl sulfate, sodium salt (SDS)-Polyacrylamide gel electrophoresis, blotted onto polyvinylidene difluoride (PVDF) membranes on ice, and blocked for 1 h at RT with 5% nonfat milk in phosphate-buffered saline (PBS). Membranes were incubated with primary antibodies (1:1000) overnight at 4 °C, washed with 0.1% Tween-20 (Gibco) PBS three times, incubated with the horseradish peroxidase-linked secondary antibody (1:2000, MBL Nagoya, Japan) for 2 h at RT, and finally visualized using Amersham ECL Prime Western blotting analysis system and imaged with a GE Healthcare Amersham imager 600 (GE Healthcare, UK). The primary antibodies of Gsdf, Igf2bp3 and β-actin are listed in Table S4.

2.5. Multi-color fluorescent immunostaining

Immunofluorescence (IF) was performed using antibodies (α-Igf2bp3 and α-H3K27me3) listed in Table S2 with gonadal sections fixed in 4% paraformaldehyde (PFA), and embedded in paraffin as described previously (Sun et al., 2017). Signals were visualized using a TSA Plus TMR/Fluorescein system (PerkinElmer Inc., Waltham, MA), following the manufacturer's instructions, and nuclei were counterstained with 4′,6-diamidino-2-phenylindole (DAPI). Results were viewed and photographed under a confocal laser scanning microscope (DMi8 TCS SP8, Leica, Germany).

3. Results

3.1. Putative downstream genes regulated by Gsdf signaling

To identify downstream genes regulated by Gsdf signaling, we compared the proteomics profiles of three adult medaka gonads: a normal XY testis, a normal XX ovary, and a *gsdf* KO ovary (Fig. 1A).

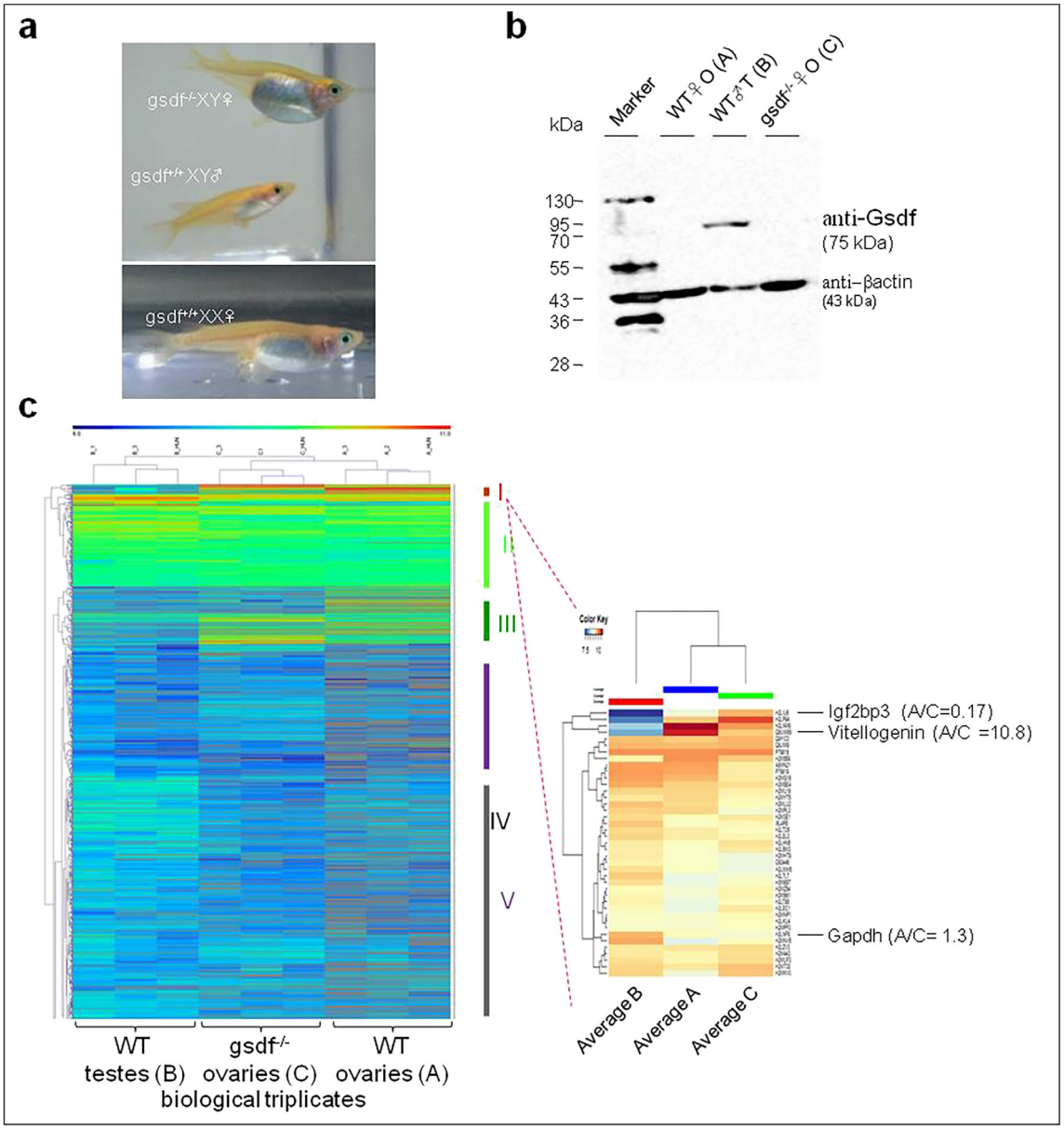

Fig. 1. Proteomic profiles of adult gonads. (a) Normal XX female, XY male, and *gsdf* KO female. (b) Western blots detected Gsdf expression in the testis but not in the normal or *gsdf* KO ovaries. (c) Heat map showing protein quantification in three biological replicates. Right panel reveals the top 41 of significantly differential proteins in the sub-cluster I, with protein details listed in Table S1. A [wild-type female (WT ovary)]; B [wild-type male (WT testis)]; and C [*gsdf* null female (gsdf$^{-/-}$ ovary)]. Pooled samples (7–10 individual gonads per group) were used to reduce the effects of individual variation.

Western blots indicated that the Gsdf protein was expressed in the normal testis only; Gsdf protein was undetectable in the normal ovary or in the *gsdf* KO ovary (Fig. 1B). After four rounds of mass spectrometry, 2556 proteins were identified in each of the three biological replicates, which were further quantified and clustered as five groups, using pairwise-comparisons to identify significantly up- or down-regulated proteins (Fig. 1C), based on the average of Exponential Means of Fold Changes derived from three biological replicates.

We identified three expression profiles in cluster I subset. The RNA-binding protein Igf2bp3 was significantly greater in the normal ovary than in the normal testis ($p < 0.0001$; a 38-fold difference; Table S1). It was further up-regulated in the *gsdf*-deficient ovary as compared to the normal ovary ($p < 0.0001$; a ~5.8-fold increase in expression; Table S1). By contrast, Vitellogenin 1 was approximately 342 times more abundant in the ovary than in testis. It decreased in the *gsdf*-deficient ovary to one tenth of the level in the normal ovary (Table S1), consistent with the histological observation that vitellogenic oocytes are rarely present in *gsdf* KO ovaries (Guan et al., 2017). House-keeping gene glyceraldehyde-3-phosphate dehydrogenase (*gapdh*), was slightly down-regulated in the *gsdf*-deficient ovary, in contrast to a four-fold higher in the normal ovary than the normal testis (Table S1).

3.2. Structural and evolutionary conservation of igf2bp3 across phyla

Medaka *igf2bp3* encodes a 586-amino-acid protein with two RNA-recognition motifs (RRMs) and four K homology (KH) domains (Fig. 2A), conserved between fish and mammals. It is distinct from insulin-like growth factor binding protein 3 (*Igfbp3*), which consists of IGFBP domain and Thyroglobulin type 1 repeats (TY), and mediates the embryo-maternal signaling necessary for embryo implantation in mammals (Fig. 2B) (Herrler et al., 2003). Medaka Igf2bp3 and human IGF2BP3 share a high amino acid similarity (> 76%) (Table S2). *igf2bp3* and neighborhood transformer 2 (*tra2*) genes are orthologous to the fruit fly (*Drosophila melanogaster*) genes IMP and *tra2,* respectively

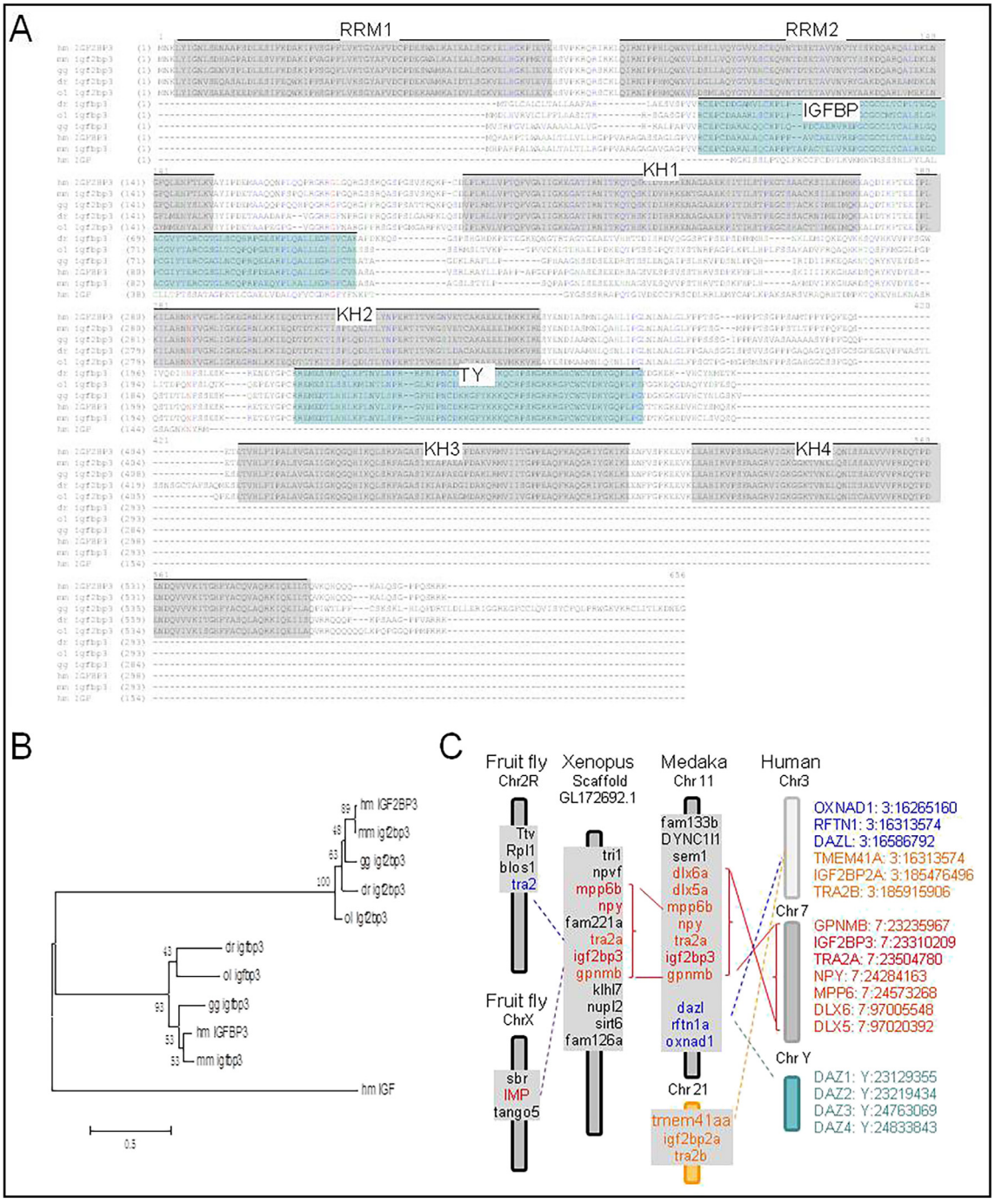

Fig. 2. Amino acid alignment and Phylogenetic relationship of Igf2bp3 and Igfbp3 across phyla. (A) Amino acid alignment was performed with CLUSTALW. Conserved domains (RRMs and KHs of Igf2bp3 homologs; IGFBP and TY of Igfbp3 homologs) are in grey and green shadows respectively. (B) Phylogenetic relationship of Igf2bp3 and Igfbp3 proteins is analyzed with Mega 6.0 program by bootstrap analysis using neighbor-joining (1000 replicates). Medaka, ol; zebrafish, dr; chicken, gg; mouse, mm; human, hm. The human IGF sequence (NM_000618.4) was used as an out-group. (C) Synteny segments flanking *igf2bp3* were well conserved across vertebrates. *tra2* and *igf2bp3* (Drosophila IMP) were located on chromosomes 2R and X ,respectively, but were tightly linked and duplicated before the segregation of vertebrates. Synteny segments are shown in red (core with *igf2bp3*); orange (duplicated in fish); blue (*Dazl* group); or light blue (*Daz*).

(Dauwalder et al., 1996; Nielsen et al., 2000). Our comparative genomic analysis indicated that Tra2 and IMP were located on separate chromosomes (2R and X, respectively) in fruit flies, but were closely linked, appear to have been duplicated as *tra2a/igf2bp3* and *tra2b/igf2bp2a* in vertebrates. Syntenic genes flanking *igf2bp3/tra2a* (Fig. 2C, in red) and *igf2bp2a/ tra2b* segments (Fig. 2C, in orange) were located on medaka chromosome 11 and 21, corresponding to segments on human chromosome 7 and 3, respectively. Notably, *dazl* gene (deleted in azoospermia like; Fig. 2C, in blue) was located close to *igf2bp3* in medaka. In humans, one copy of *dazl* was located on human chromosome 3 near IGF2BP2A, while the other copy was translocated onto the Y chromosome to become DAZ (Fig. 2C, in light blue), only found in old world monkeys and hominids (Saxena et al., 1996).

3.3. Predominant expression of igf2bp3 in the developmental ovary

To explore the role of *igf2bp3* in gonad development, the cDNA of *igf2bp3* was sub-cloned using specific primers for this study (based on

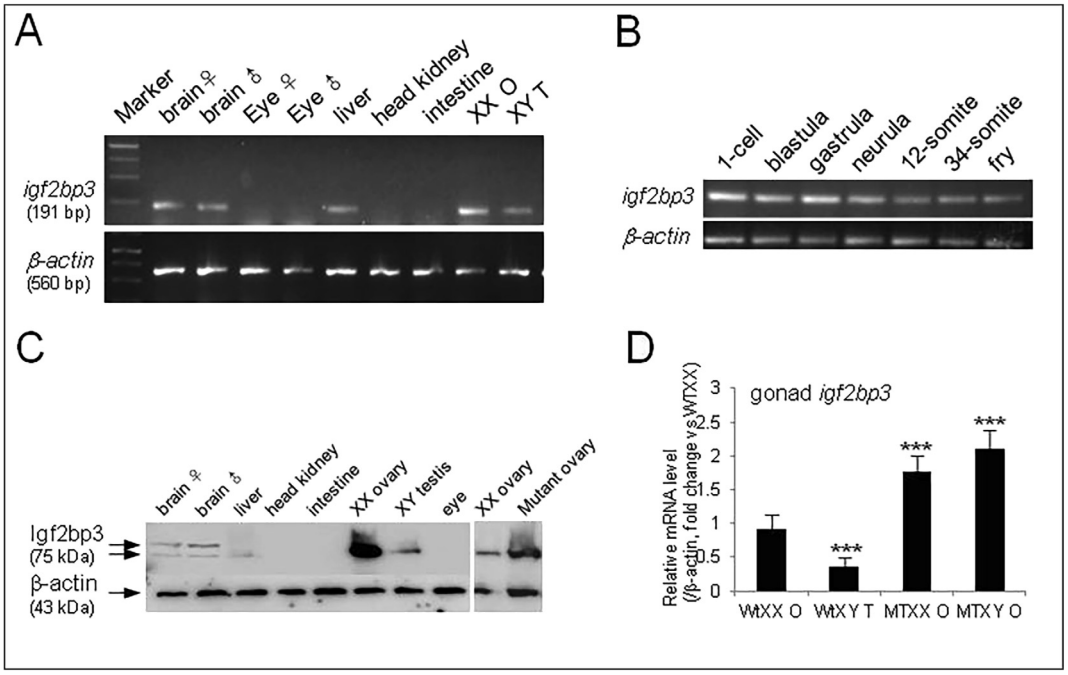

Fig. 3. Spatio-temporal expression profiles of *igf2bp3*. (A) *igf2bp3* expression is detectable in brain, liver, ovary and testis by RT-PCR. (B) *igf2bp3* transcripts persist throughout embryogenesis by RT-PCR analysis. (C) Igf2bp3 protein is predominantly expressed in ovary, slightly in liver and testis. An additional isoform of Igf2bp3 is only detected in female and male brains. Igf2bp3 protein expression is higher in *gsdf* KO XY ovary than normal ovary detected by Western blot (right panel). (D) Comparison of *igf2bp3* transcripts among the wild-type ovary (WT XX), wild-type testis (WT XY), and homozygous ovary (MT XX and MT XY gsdf$^{-/-}$) by quantitative PCR analyses. Relative mRNA expression was normalized against β-actin in gonads. Vertical bars represent means ± SEM (n = 6). Asterisks indicate significant differences compared to WT XX.

database from ensembl.org/Oryzias_latipes/Gene; HdrR strain ASM223467v1; Table S3). *igf2bp3* transcripts were detectable in medaka brain, liver, and testis/ovary, but was not expressed in the eye, head kidney, and intestine by RT-PCR analysis (Fig. 3A). *igf2bp3* was expressed throughout embryogenesis (Fig. 3B). Using Western blot, we detected an extra fragment of Igf2bp3 in the adult brain, in addition to the common Igf2bp3 fragment identified in the liver and gonad. This suggested that a different Igf2bp3 isoform was likely generated by post-translational modifications in the central nervous system of the medaka (Fig. 3C). It was reported an expression of *igf2bp3* orthologue in the fetal central nervous systems of mice and fruit flies (Mori et al., 2001; Nielsen et al., 2000), but decreased to be undetectable in adult brain in mice (Mori et al., 2001). The abundance of protein products was highest in the *gsdf* KO ovary, followed by the normal ovary, and the testis (Fig. 3C), consistent with the results from our proteomics analysis (Fig. 1C). qPCR also identified a greater abundance of transcripts in the *gsdf* KO ovary (Fig. 3D). The high levels of *igf2bp3* expression in the medaka ovary were consistent with the expression of the orthologous gene Vg1RBP/Vera, which is critical for mRNA polarization in *Xenopus laevis* oogenesis (Deshler et al., 1998). In contrast to lower vertebrates, mammalian *igf2bp3* is highly expressed in mouse and human testes, but weakly expressed in ovaries (Hammer et al., 2005; Mori et al., 2001; Shantha Kumara et al., 2015).

3.4. Dynamic expression of H3K27Bp3 and Igf2bp3 in gonad during early oogenesis

The gonads are morphologically similar in early XX and XY embryos, but are distinct during the hatching stage when germ cells enter meiosis in female ovary (Nishimura et al., 2016). Signals of anti-Igf2bp3 antibodies were detectable in the nucleus of zygotene oocytes (based on morphological evaluation) in normal XX, during the hatching stage by IF (Fig. 4a, an enlarged image in 4a′). It was co-localized with H3K27me3, one of oogonia meiotic entry markers also found in mouse oogenesis (Fu et al., 2017). Gsdf was detectable in somatic cells surrounding oocytes in normal ovaries at 15-dah stage, different from the Igf2bp3 signals around chromosomes of prophase oocytes (Fig. 4b-b′). Signals of Igf2bp3 and H3K27me3 were transferred from chromosomes to perinuclear area of oocytes at stage of 25-dah (Fig. 4c, an enlarged image in 4c′). The specificity of IF signals was verified as the absence of any signals in sections without primary antibodies, which served as negative controls (Fig. 4b″ and c″).

3.5. Cystic cell proliferation activated abundantly in 1-month-old gsdf-deficient ovary

Igf2bp3 expression was transferred from the nucleus of zygotene germ cells to the cytoplasm of primary oocytes in 1-month-old ovary of normal and *gsdf* KO females (Figs. 4 and 5). In medaka, germ cells commit two types of division during development: a self-renewal division (type I), and a synchronously and successively division to enter meiosis (type II) (Nishimura et al., 2014). Germ cells enter meiosis after a cystic division (type II division) by the hatching stage in female, or keep type I division in male until 1-month later to initiate type II division and subsequently enter spermatogenesis (Nishimura et al., 2014). However, we were surprised to observe that numerous type II cystic germ cells accumulated in one-month-old of *gsdf* deleted ovary, the phenomenon rarely observed in normal ovary (Fig. 5). Many cysts were composed of 2- (Fig. 5a1 **asterisk) to 8-synchronized type II cells positive to both Igf2bp3 and H3K27me3 antisera (Fig. 5a and an enlarged image in 5a1). A few of cysts were even composed of asynchronous germ cells with both Igf2bp3/H3K27me3 positive and negative germ cells inside one cyst (Fig. 5b and 5b1). Morphological evaluation of these germ cells was confirmed by hematoxylin and eosin (HE) staining shown in Fig. S1a-a2 and Fig. S1b-b2 respectively. Seven germ cells (No 2–8 in Fig. 5b-b1) negative to Igf2bp3/H3K27me3 antibodies were probably type I self renewal germ cells with a clear nucleolus. No. 1 (a pachytene like germ cell in Fig. 5b1 and Fig. S1b-b2)

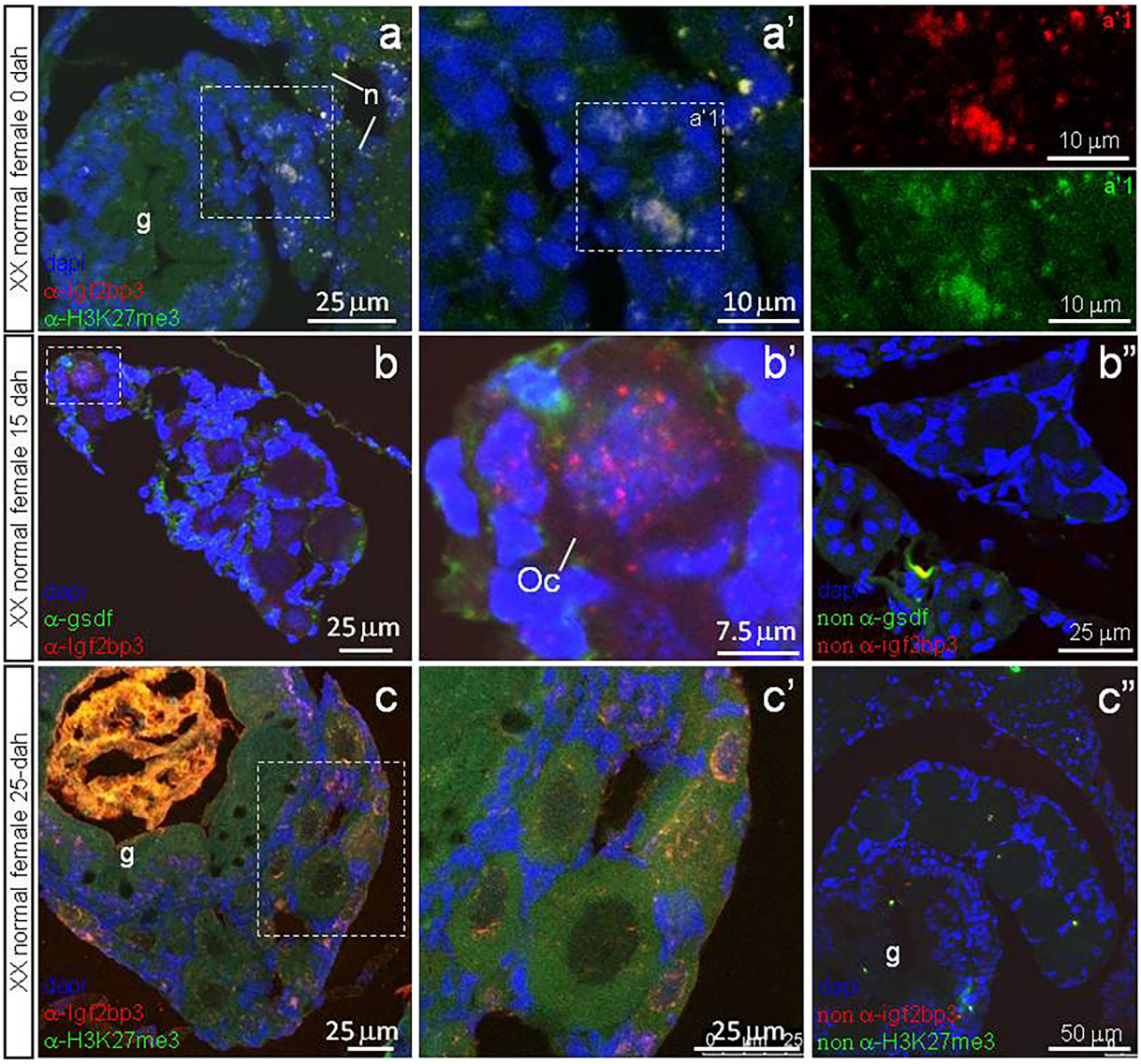

Fig. 4. Dynamic expression of H3K27me3 and Igf2bp3 during ovarian development. Protein expression was detected by IF in cross-sections of normal XX ovaries at 0 dah (a), 15 dah (b) and 25 dah (c), using antibodies of anti-H3K27me3 (in green), or anti-Gsdf (in green) and anti-Igf2bp3 (in red) respectively. Magnified images are present in a′, b′ and c′ respectively. a1′ red and green are single channels of a1 frame in a'. As a negative control, no signals were detected in cross sections at 15 dah (b″) and (c″) without primary anti-Igf2bp3 and anti-H3K27me3 antibodies. n: nephric duct; g: hindgut; Oc: oocyte.

was negative to both Igf2bp3 and H3K27me3 antisera reaction, showing the clear appearance of the meiotic chromosomes' condensation and pairing. These results indicated the existence of at least two populations of germ cells during mitosis to meiosis transition within the same cyst, which were distinct from each other by the presence of Igf2bp3 and H3K27me3. By contrast, the protein translation of Igf2bp3 and H3K27me3 was apparently less in normal oocyte than *gsdf* KO oocytes (Fig. 5c-c1), consistent with the results from proteomics analysis. A few of synchronous germ cells were observed in the normal 1-month ovary (Fig. 5d). The presence of heterogeneous germ cells in one cyst was observed in all three *gsdf* KO XY ovaries (Fig. S2), but not in normal XX ovaries (n = 4), nor *gsdf* KO XX individuals (n = 3) being checked (data unpublished), indicating this type of asynchronous cysts were probably only present in *gsdf* KO XY ovaries. The number of primary oocytes in *gsdf* KO XY ovary is about 1.5 times that of normal XX ovary at one-month-old stage (the ratio of 76.8 to 49.9 in Fig. 5e). Metaphase I oocytes increased significantly to one forth of total primary oocytes in *gsdf* KO XY ovary, by contrast to the one tenth of total primary oocytes in normal XX ovary (Fig. 5e). Therefore, we concluded that the irregular accumulation of excessive primary oocytes in the *gsdf* deficient ovary was probably resulted from the abnormal increase of cystic division and proliferation, caused by in the shortage of Gsdf signaling.

4. Discussion

In this study, we identified an Igf2bp3-mediated pathway, regulated by Gsdf, which was involved in oocyte development. Our proteomics-based comparison of *gsdf*-intact and *gsdf*-null mutant gonads indicated that Igf2bp3 protein expression was dramatically elevated in the *gsdf*-deficient ovary. Importantly, primary oocytes within numerous cysts highly expressed Igf2bp3/H3K27me3 at zygotene and pachytene stages. Both Igf2bp3/H3K27me3 positive and negative germ cells were observed in 1-month-old *gsdf*-deficient ovary. In contrast to gonocyte type II division followed by spermatogenesis usually occurs in 1-month-old testis in medaka (Nishimura et al., 2014), type II cysts were scarcely found in 1-month-old normal ovary. This result revealed the oocyte heterogeneity with respect to the protein expression of *igf2bp3*. Interestingly, oocyte heterogeneity has also been reported in XY sex-reversed mouse as the result of unsynapsed XY chromosomes (Taketo

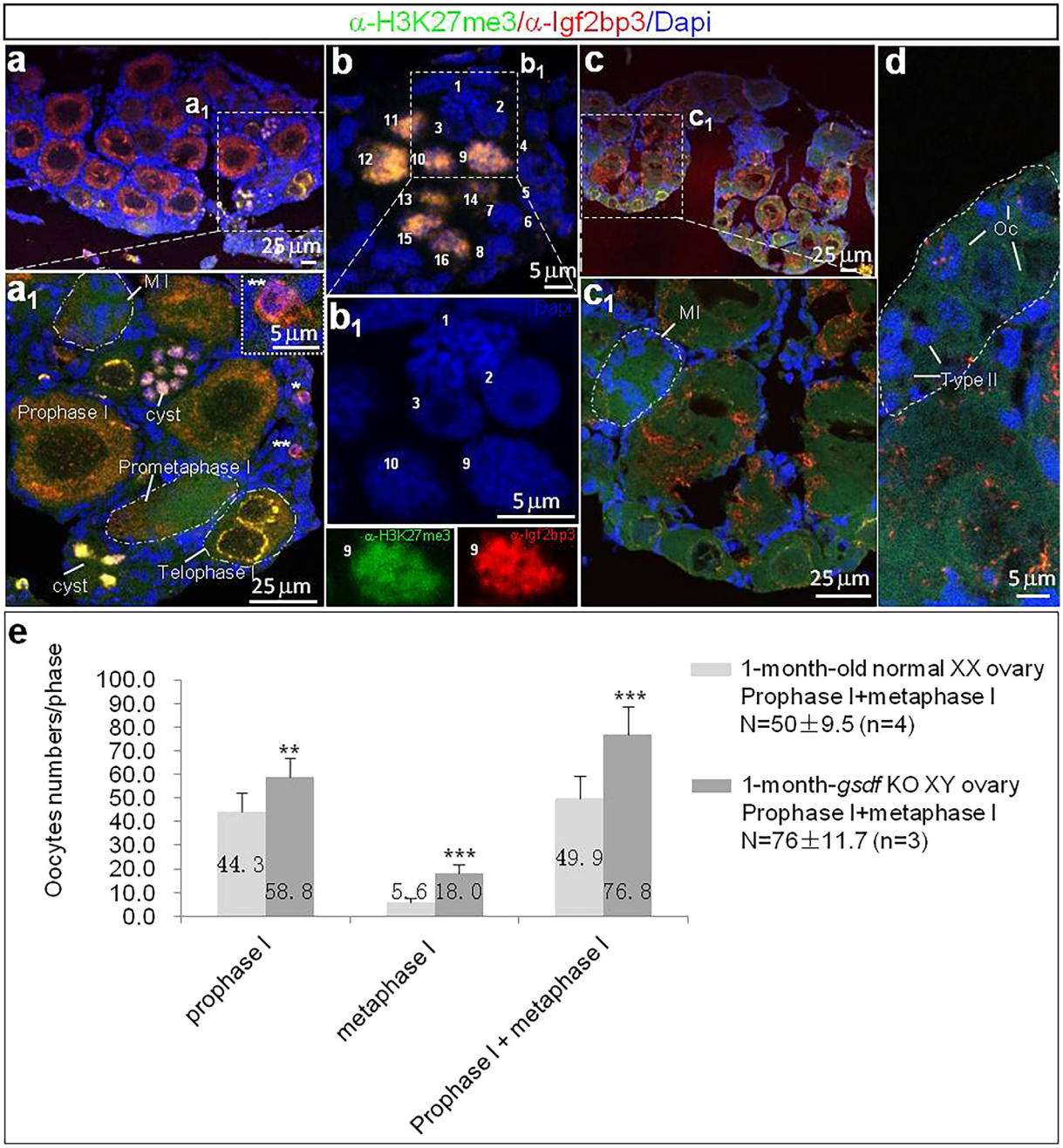

Fig. 5. Loss of *gsdf* led to a dysregulation of Igf2bp3-mediated oocyte development. Cross sections of 1-month-old *gsdf* KO (a-b) and wild-type ovaries (c to d) were subjected to multi-color IF analysis using antibodies of Igf2bp3 (in red) and H3K27me3 (in green). Nucleus was counterstained with Dapi (in blue). Abundant cysts composed of Igf2bp3/ H3K27me3 positive germ cells were detected in *gsdf* KO ovary (a-b, the magnified images a1-b1, three color channels of b1). The germinal cradle in wild-type ovary was encircled by a dotted line (d). * and ** stand for single and double Igf2bp3-positive mitotic germ cells (a1); Oc: oocyte; M I: meiotic metaphase I. (e) Number of meiotic oocytes (prophase I and metaphase I) were counted per section with two phases randomly collected from four individuals of normal ovaries (n = 4), and three *gsdf* KO XY ovaries (n = 3). The asterisks indicated significant differences compared to the normal $gsdf^{+/+}$ ovaries (**$p < 0.01$, ***$p < 0.001$).

et al., 2013). It was noteworthy that H3K27me3 is known to be associated with repression of gene expression and genomic imprinting at the X chromosome inactivation-specific transcript (*Xist)* and *IGF2* loci (Dindot et al., 2004; Inoue et al., 2017). Maternal H3K27me3 has been shown to coat *Xist* locus and is responsible for maternal *Xist* silencing in mouse (Inoue et al., 2017). It might be possible that H3K27me3 was activated and necessary for meiotic silencing of unsynapsed XY regions in medaka as well, assuming that H3K27me3 plays the similar role of genomic imprinting in medaka as it plays in mouse. The enrichment of Igf2bp3 on condensed chromosomes, suggesting its potential involvement in the synthesis inhibition or degradation of specific mRNAs associated with chromosomal pairing and homologous recombination.

In medaka, transplantation of XY somatic cells is sufficient to induce spermatogenesis in female XX medaka (Shinomiya et al., 2002), thus demonstrated that gonadal somatic cells play the dominant role in determining the sexual fate of germ cells. It was not surprising that oocyte was developed as a result of switching off the somatic male pathway by *gsdf* depletion. Higher expression of *gsdf* in Sertoli cells surrounding type A spermatogonia in XY during gonadal sex

differentiation, suggesting the potential role of *gsdf* in the transition of type I and type II division (Nishimura et al., 2014; Shibata et al., 2010). It was noted that abundant cysts with type II cystic division present abnormally in 1-month-old in *gsdf* deficient ovaries, supporting the repression of type II cystic division under the regulation of Gsdf signaling. It was possible that those Igf2bp3 expressing oocytes within the cysts of *gsdf* deficient ovary might retain somewhat male features, and therefore failed to grow normally in the absence of *gsdf* or other somatic factors. As a result, an excessive primary oocyte accumulation was shown in the adult ovary.

In summary, we identified a novel mechanism of Gsdf/Igf2bp3 regulation during medaka germ cell development. The similar pattern of expression identified in medaka and *Xenopus* suggested that Igf2bp3 plays an important role in oocyte development, which is conserved across the lower vertebrates. Functional analyses of Igf2bp3 will provide further insights into the mechanisms underlying the onset of oogenesis and spermatogenesis in medaka, which may be conserved across phyla.

Acknowledgments

This work was supported by the Shanghai University First-Class Disciplines Project of Fisheries and the International Research Group Program; a grant was given to GG from the Shanghai Municipal Natural Science Foundation China (16ZR1415200), and grant was given to ZX from the National Natural Science Foundation of China (81771545). We thank the Beijing Bangfei Bioscience Co., Ltd (Beijing, China) for technical expertise in proteomics. We also thank Accdon (www.accdon.com) for providing language editing services.

Competing interests

The authors declare that they have no competing interests.

The authors declare that the research was conducted in the absence of any commercial or financial relationships that could be construed as potential conflicts of interest.

Authors' contributions

Conceptualization, GG and ZX; Methodology, GG and HX; Investigation, GG, XW, SX, YZ, AG, HG, YY, YK; Writing-Original Draft, GG and SX; Writing-Review & Editing, GG, LC and LetPub; Funding Acquisition, GG, LC, and XZ; Supervision, GG, LC, and XZ.

Appendix A. Supplementary data

Supplementary data to this article can be found online at https://doi.org/10.1016/j.ygcen.2019.04.001.

References

Dauwalder, B., Amaya-Manzanares, F., Mattox, W., 1996. A human homologue of the Drosophila sex determination factor transformer-2 has conserved splicing regulatory functions. Proc. Natl. Acad. Sci. U.S.A. 93, 9004–9009.
Deshler, J.O., Highett, M.I., Abramson, T., Schnapp, B.J., 1998. A highly conserved RNA-binding protein for cytoplasmic mRNA localization in vertebrates. Curr. Biol. 8, 489–496.
Dindot, S.V., Kent, K.C., Evers, B., Loskutoff, N., Womack, J., Piedrahita, J.A., 2004. Conservation of genomic imprinting at the XIST, IGF2, and GTL2 loci in the bovine. Mamm Genome. 15, 966–974.
Fu, X.F., Yang, F., Cheng, S.F., Feng, Y.N., Li, L., Dyce, P.W., et al., 2017. The epigenetic modifications and the anterior to posterior characterization of meiotic entry during mouse oogenesis. Histochem. Cell Biol. 148, 61–72.
Guan, G., Sun, K., Zhang, X., Zhao, X., Li, M., Yan, Y., et al., 2017. Developmental tracing of oocyte development in gonadal soma-derived factor deficiency medaka (Oryzias latipes) using a transgenic approach. Mech. Dev. 143, 53–61.
Hammer, N.A., Hansen, T., Byskov, A.G., Rajpert-De, Meyts E., Grondahl, M.L., Bredkjaer, H.E., et al., 2005. Expression of IGF-II mRNA-binding proteins (IMPs) in gonads and testicular cancer. Reproduction 130, 203–212.
Herrler, A., von Rango, U., Beier, H.M., 2003. Embryo-maternal signalling: how the embryo starts talking to its mother to accomplish implantation. Reprod. Biomed. Online 6, 244–256.
Imai, T., Saino, K., Matsuda, M., 2015. Mutation of Gonadal soma-derived factor induces medaka XY gonads to undergo ovarian development. Biochem. Biophys. Res. Commun. 467, 109–114.
Inoue, A., Jiang, L., Lu, F., Zhang, Y., 2017. Genomic imprinting of Xist by maternal H3K27me3. Genes Dev. 31, 1927–1932.
Matsuda, M., Nagahama, Y., Shinomiya, A., Sato, T., Matsuda, C., Kobayashi, T., et al., 2002. DMY is a Y-specific DM-domain gene required for male development in the medaka fish. Nature 417, 559–563.
Mori, H., Sakakibara, S., Imai, T., Nakamura, Y., Iijima, T., Suzuki, A., et al., 2001. Expression of mouse igf2 mRNA-binding protein 3 and its implications for the developing central nervous system. J. Neurosci. Res. 64, 132–143.
Morinaga, C., Saito, D., Nakamura, S., Sasaki, T., Asakawa, S., Shimizu, N., et al., 2007. The hotei mutation of medaka in the anti-Mullerian hormone receptor causes the dysregulation of germ cell and sexual development. Proc. Natl. Acad. Sci. U.S.A. 104, 9691–9696.
Murozumi, N., Nakashima, R., Hirai, T., Kamei, Y., Ishikawa-Fujiwara, T., Todo, T., et al., 2014. Loss of follicle-stimulating hormone receptor function causes masculinization and suppression of ovarian development in genetically female medaka. Endocrinology 155, 3136–3145.
Nanda, I., Kondo, M., Hornung, U., Asakawa, S., Winkler, C., Shimizu, A., et al., 2002. A duplicated copy of DMRT1 in the sex-determining region of the Y chromosome of the medaka, Oryzias latipes. Proc. Natl. Acad. Sci. U.S.A. 99, 11778–11783.
Nielsen, J., Cilius, Nielsen F., Kragh, Jakobsen R., Christiansen, J., 2000. The biphasic expression of IMP/Vg1-RBP is conserved between vertebrates and Drosophila. Mech. Dev. 96, 129–132.
Nishimura, T., Sato, T., Yamamoto, Y., Watakabe, I., Ohkawa, Y., Suyama, M., et al., 2015. Sex determination. foxl3 is a germ cell-intrinsic factor involved in sperm-egg fate decision in medaka. Science 349, 328–331.
Nishimura, T., Nakamura, S., Tanaka, M., 2016. A Structurally and functionally common unit in testes and ovaries of medaka (Oryzias latipes), a teleost fish. Sex Dev. 10, 159–165.
Nishimura, T., Tanaka, M., 2014. Gonadal development in fish. Sex Dev. 8, 252–261.
Nishimura, T., Yamada, K., Fujimori, C., Kikuchi, M., Kawasaki, T., Siegfried, K.R., et al., 2018. Germ cells in the teleost fish medaka have an inherent feminizing effect. PLoS Genet. 14, e1007259.
Saxena, R., Brown, L.G., Hawkins, T., Alagappan, R.K., Skaletsky, H., Reeve, M.P., et al., 1996. The DAZ gene cluster on the human Y chromosome arose from an autosomal gene that was transposed, repeatedly amplified and pruned. Nat. Genet. 14, 292–299.
Shantha, Kumara H., Kirchoff, D., Caballero, O.L., Su, T., Ahmed, A., Herath, S.A., et al., 2015. Expression of the cancer testis antigen IGF2BP3 in colorectal cancers; IGF2BP3 holds promise as a specific immunotherapy target. Oncoscience 2, 607–614.
Sheng, Y., Zhao, W., Song, Y., Li, Z., Luo, M., Lei, Q., et al., 2015. Proteomic analysis of three gonad types of swamp eel reveals genes differentially expressed during sex reversal. Sci. Rep. 5, 10176.
Shibata, Y., Paul-Prasanth, B., Suzuki, A., Usami, T., Nakamoto, M., Matsuda, M., et al., 2010. Expression of gonadal soma derived factor (GSDF) is spatially and temporally correlated with early testicular differentiation in medaka. Gene Expr. Patterns 10, 283–289.
Shinomiya, A., Shibata, N., Sakaizumi, M., Hamaguchi, S., 2002. Sex reversal of genetic females (XX) induced by the transplantation of XY somatic cells in the medaka, Oryzias latipes. Int. J. Dev. Biol. 46, 711–717.
Sun, K., Fan, L., Wang, C., Yang, X., Zhu, S., Zhang, X., et al., 2017. Loss of gonadal soma derived factor damaging the pituitary-gonadal axis in medaka. Sci. Bull. 62, 159–161.
Takahashi, A., Kanda, S., Abe, T., Oka, Y., 2016. Evolution of the hypothalamic-pituitary-gonadal axis regulation in vertebrates revealed by knockout medaka. Endocrinology 157, 3994–4002.
Taketo, T., Naumova, A.K., 2013. Oocyte heterogeneity with respect to the meiotic silencing of unsynapsed X chromosomes in the XY female mouse. Chromosoma 122, 337–349.
Zhang, X., Guan, G.J., Li, M.Y., Zhu, F., Liu, Q.Z., Naruse, K., et al., 2016. Autosomal gsdf acts as a male sex initiator in the fish medaka. Sci. Rep-UK 6.
Zhu, W., Smith, J.W., Huang, C.M., 2010. Mass spectrometry-based label-free quantitative proteomics. J. Biomed. Biotechnol. 2010, 840518.
Zhu, Y., Wang, C., Chen, X., Guan, G., 2016. Identification of gonadal soma-derived factor involvement in Monopterus albus (protogynous rice field eel). Mol. Biol. Rep.